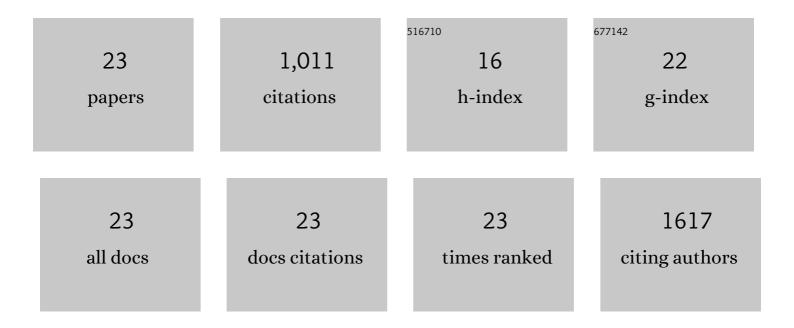
Marko Pesola

List of Publications by Year in descending order

Source: https://exaly.com/author-pdf/4270756/publications.pdf Version: 2024-02-01



MADKO PESOLA

#	Article	IF	CITATIONS
1	Convergence of supercell calculations for point defects in semiconductors: Vacancy in silicon. Physical Review B, 1998, 58, 1318-1325.	3.2	233
2	Computational study of interstitial oxygen and vacancy-oxygen complexes in silicon. Physical Review B, 1999, 60, 11449-11463.	3.2	103
3	Radiomics and machine learning of multisequence multiparametric prostate MRI: Towards improved non-invasive prostate cancer characterization. PLoS ONE, 2019, 14, e0217702.	2.5	76
4	Evaluation of different mathematical models for diffusion-weighted imaging of normal prostate and prostate cancer using high b-values: A repeatability study. Magnetic Resonance in Medicine, 2015, 73, 1988-1998.	3.0	72
5	Prospective evaluation of 18F-FACBC PET/CT and PET/MRI versus multiparametric MRI in intermediate- to high-risk prostate cancer patients (FLUCIPRO trial). European Journal of Nuclear Medicine and Molecular Imaging, 2018, 45, 355-364.	6.4	66
6	Mathematical models for diffusionâ€weighted imaging of prostate cancer using b values up to 2000 s/mm ² : Correlation with Gleason score and repeatability of region of interest analysis. Magnetic Resonance in Medicine, 2015, 74, 1116-1124.	3.0	53
7	Fitting methods for intravoxel incoherent motion imaging of prostate cancer on region of interest level: Repeatability and gleason score prediction. Magnetic Resonance in Medicine, 2017, 77, 1249-1264.	3.0	48
8	MR signal-fat-fraction analysis and T2* weighted imaging measure BAT reliably on humans without cold exposure. Metabolism: Clinical and Experimental, 2017, 70, 23-30.	3.4	48
9	Serum levels of GFAP and EGFR in primary and recurrent high-grade gliomas: correlation to tumor volume, molecular markers, and progression-free survival. Journal of Neuro-Oncology, 2015, 124, 237-245.	2.9	42
10	Spin-density study of the silicon divacancy. Physical Review B, 1998, 58, 1106-1109.	3.2	41
11	Optimization of b-value distribution for biexponential diffusion-weighted MR imaging of normal prostate. Journal of Magnetic Resonance Imaging, 2014, 39, 1213-1222.	3.4	37
12	Vibrations of the Interstitial Oxygen Pairs in Silicon. Physical Review Letters, 1999, 82, 4022-4025.	7.8	36
13	Diffusion-weighted imaging of prostate cancer: effect of b-value distribution on repeatability and cancer characterization. Magnetic Resonance Imaging, 2015, 33, 1212-1218.	1.8	23
14	Assessment of dosimetric and positioning accuracy of a magnetic resonance imaging-only solution for external beam radiotherapy of pelvic anatomy. Physics and Imaging in Radiation Oncology, 2019, 11, 1-8.	2.9	23
15	Repeatability of radiomics and machine learning for DWI: Shortâ€ŧerm repeatability study of 112 patients with prostate cancer. Magnetic Resonance in Medicine, 2020, 83, 2293-2309.	3.0	23
16	Somatostatin receptor subtype 2 in high-grade gliomas: PET/CT with 68Ga-DOTA-peptides, correlation to prognostic markers, and implications for targeted radiotherapy. EJNMMI Research, 2015, 5, 25.	2.5	20
17	Rotating frame relaxation imaging of prostate cancer: Repeatability, cancer detection, and Gleason score prediction. Magnetic Resonance in Medicine, 2016, 75, 337-344.	3.0	16
18	Relaxation along fictitious field, diffusion-weighted imaging, and T ₂ mapping of prostate cancer: Prediction of cancer aggressiveness. Magnetic Resonance in Medicine, 2016, 75, 2130-2140.	3.0	15

Marko Pesola

#	Article	IF	CITATIONS
19	Validation of automated magnetic resonance image segmentation for radiation therapy planning in prostate cancer. Physics and Imaging in Radiation Oncology, 2020, 13, 14-20.	2.9	14
20	Microscopic structure of oxygen defects in gallium arsenide. Physical Review B, 1999, 60, R16267-R16270.	3.2	12
21	Diffusion weighted imaging of prostate cancer: Prediction of cancer using texture features from parametric maps of the monoexponential and kurtosis functions. , 2016, , .		6
22	Prediction of prostate cancer aggressiveness using 18F-Fluciclovine (FACBC) PET and multisequence multiparametric MRI. Scientific Reports, 2020, 10, 9407.	3.3	3
23	Whole Brain Adiabatic T 1rho and Relaxation Along a Fictitious Field Imaging in Healthy Volunteers and Patients With Multiple Sclerosis: Initial Findings. Journal of Magnetic Resonance Imaging, 2021, 54, 866-879.	3.4	1